Scott, R. A., and Scheraga, H. A. (1963), *J. Am. Chem. Soc. 85*, 3866.
Shechter, E., and Blout, E. R. (1964), *Proc. Natl. Acad. Sci. U. S. 51*, 794.
Singer, S. J. (1962), *Advan. Protein Chem. 17*, 1.
Sophianopoulos, A. J., Rhodes, C. K., Holcomb, D. N., and Van Holde, K. E. (1962), *J. Biol. Chem. 237*, 1107.
Tanford, C. (1962), *J. Am. Chem. Soc. 84*, 1747.
Urnes, P., and Doty, P. (1961), *Advan. Protein Chem. 16*, 401.
Weber, R. E., and Tanford, C. (1959), *J. Am. Chem. Soc. 81*, 3255.
Wilcox, P. E., Cohen, E., and Neurath, H. (1957), *J. Biol. Chem. 228*, 999.
Williams, E. J., Herskovits, T. T., and Laskowski, Jr., M. (1965), *J. Biol. Chem. 240*, 3580.

Shell Model Calculations of Rotational Diffusion Coefficients*

Don P. Filson and Victor A. Bloomfield

ABSTRACT: Previous work has shown that it is possible to calculate the translational frictional coefficient of a complex structure by modelling the structure by a surface shell of spherical frictional elements. The shell model is here employed to calculate the rotational diffusion coefficients ($D^{\theta\theta}$) of structures with cylindrical symmetry, using theoretical formulations of Kirkwood and Hearst. Kirchoff's law for a sphere is obtained exactly, while $D^{\theta\theta}$'s calculated by this method are high by 8% or less compared to the exact Perrin results for prolate ellipsoids of revolution. Fair agreement with experiment on tobacco mosaic virus is obtained without explicitly introducing end effects in cylinders, which are shown to be small. The extension of tail fibers is shown to be necessary to obtain the $D^{\theta\theta}$ observed for the fast form of T2 bacteriophage by Maestre, if electron microscopic dimensions for the virus are used; but uniform expansion of the head by nearly a factor of two, or lengthening by a factor of three, is necessary to explain that observed for the slow form. Methods for extrapolation to a continuous surface distribution are discussed. It has been found empirically that coarse modelling of the surface, followed by shrinkage of the radii of the frictional elements by 50%, gives in all cases investigated a value of $D^{\theta\theta}$ which is within 6% of the shell model value.

Rotational diffusion coefficients, measured, for example, by flow or electrical birefringence or dichroism, or by fluorescence depolarization, provide an important source of information on the size and shape of macromolecules. In order for these coefficients to be interpreted, their dependence on size and shape for a model closely resembling the structure actually under study must be understood. The hydrodynamic models which have been studied theoretically up to now are ellipsoids of revolution (Gans, 1928; Perrin, 1934), rigid rods (Burgers, 1938; Broersma, 1960), random coils (Zimm, 1956), and wormlike chains of intermediate flexibility (Hearst, 1963). However, this range of structures by no means exhausts those encountered experimentally. In particular, many viruses have structures of considerable complexity, and it has seemed worthwhile to attempt to extend the methods of calculation of hydrodynamic properties to be able to deal with these more complex possibilities.

The basic theoretical foundation from which this extension takes place is Kirkwood's (1949, 1954; Riseman and Kirkwood, 1956) theory of irreversible processes in solutions of macromolecules. This theory treats macromolecules as being composed of identical frictional elements. Hearst (1963) has used the Kirkwood theory to obtain explicit expressions for the components of the rotational diffusion coefficient tensor (D) for a distribution of elements having cylindrical symmetry.

Previous work (Bloomfield *et al.*, 1967) has demonstrated that the Kirkwood theory can be combined with a particular method of modelling by small frictional elements to calculate with good accuracy the translational frictional coefficients of large structures of quite arbitrary shape. This method of modelling, called the "shell model," represents a particle of given shape by an assembly of small spherical frictional elements covering a surface of that shape. The hydrodynamic properties of the assembly of frictional elements will be close to those

* From the Department of Chemistry and Chemical Engineering, University of Illinois, Urbana, Illinois 61801. *Received February 13, 1967.* This study was supported in part by a grant from the U. S. Public Health Service (GM 12555) and by a grant from the National Science Foundation (GP 700). A preliminary account of this work was presented to the Division of Polymer Chemistry at the 153rd National Meeting of the American Chemical Society, Miami Beach, Fla., April 1967. This paper is taken from a thesis of D. P. F. submitted in partial fulfillment of the requirements for a Ph.D. degree at the University of Illinois, 1967.

of the particle of interest, and will approach them more and more closely as the size of the elements in the shell is decreased while their number is increased, thereby passing to a continuous surface shell. It was shown that this approach gave Stoke's law for the translational frictional coefficients of spheres, agreed to better than 4% with the exact results of Perrin (1936) for ellipsoids of revolution, and gave useful results for the translational behavior of viruses of complex structure. In this communication, the shell model approach is used to calculate rotational diffusion coefficients for spheres and ellipsoids, to examine end effects on the rotational behavior of tobacco mosaic virus (TMV) (Broersma, 1960), and to interpret electrical birefringence studies (Maestre, 1966) on T2 bacteriophage. This approach is very well adapted to use of digital computers.

Method of Calculation

Basic Equation. The equation used for computation of rotational diffusion coefficients $D^{\theta\theta}$ is that derived by Hearst (1963)

$$\frac{D^{\theta\theta}}{kT} = \frac{1}{(\alpha+\beta)\zeta}\left\{1 + \frac{\zeta}{8\pi\eta_0(\alpha+\beta)}\sum_{s=1}^{N}{\sum_{t=1}^{N}}'\left[\left\langle\frac{l_s l_t}{R_{st}}\right\rangle + \left\langle\frac{n_s n_t}{R_{st}}\right\rangle + \left\langle\frac{(l_s n_t - n_s l_t)^2}{R_{st}^3}\right\rangle\right]\right\} \quad (1)$$

where l_s, m_s, and n_s are the particle-fixed Cartesian coordinates of element s, n_s being measured along the cylindrical axis.

$$\alpha = \sum_{s=1}^{N}\langle l_s^2\rangle, \qquad \beta = \sum_{s=1}^{N}\langle n_s^2\rangle \quad (2)$$

ζ is the translational frictional coefficient of each element, and equals $6\pi\eta_0 r$ for spheres, where η_0 is the solvent viscosity and r the sphere radius; N is the number of frictional elements modelling the structure; R_{st} is the distance between elements s and t; and the prime on the double sum denotes omission of the terms with s = t. The angular brackets denote averaging over the internal coordinates of the particle, which for the rigid structures considered here is unnecessary.

Extrapolation. For any given assembly of frictional elements representing a particle of given shape, $D^{\theta\theta}$ may be calculated using eq 1 and 2. A new assembly may be established by reducing the element radius r, so that a greater number of elements is necessary to represent the particle, and $D^{\theta\theta}$ again calculated. In this way a number of (r, $D^{\theta\theta}$) "data points" may be accumulated. The continuous shell model value of $D^{\theta\theta}$ may then be obtained by extrapolation to $r = 0$.

In order for this extrapolation to be carried out with confidence, something should be known about the functional dependence of $D^{\theta\theta}$ on r. Bloomfield *et al.* (1967) assumed that frictional elements placed with their centers on a spherical surface of radius R_0 would increase the effective hydrodynamic radius of the particle by a factor proportional to r.

$$R_{eff} = R_0 + \beta' r \quad (3)$$

Then the translational frictional coefficient is

$$f = 6\pi\eta_0 R_{eff} \quad (4)$$

f is, therefore, expected to be a linear function of r, so that the shell model value of f should be accurately obtained by linear extrapolation. The numerical value of β' was 0.25, as determined from plots of calculated points. Modelling of nonspherical particles presents a more complicated picture, since β' might be a function of position, but in practice a linear extrapolation was found to be adequate in all cases.

The situation is less favorable for extrapolation of rotational diffusion calculations. In this case there is a cubic dependence of rotational frictional coefficient ζ_r on radius for spherical particles

$$\zeta_r = kT/D^{\theta\theta} = 8\pi\eta R^3 \quad (5)$$

This means that a linear extrapolation of calculations cannot be justified; and it also means that a given increase in effective hydrodynamic radius will have a larger effect on ζ_r than on f, so that it is more important to guide the extrapolation properly. If R_{eff} given by eq 3 is substituted into eq 5, a cubic extrapolation seems appropriate. On this assumption, $D^{\theta\theta}$ can be represented as a power series in r, and it seems plausible that this series can be truncated with sufficient accuracy beyond the term in r^3 so that a cubic extrapolation of $D^{\theta\theta}$ *vs.* r should also be effective.

For nonspherical assemblies of frictional elements, the situation is again more complex. For a prolate ellipsoid of revolution with axial ratio $p = a_1/a_2$ (Perrin, 1934)

$$\zeta_r = 8\pi\eta_0 a_1 a_2^2/y(p) \quad (6)$$

where

$$y(p) = \frac{3}{2}\frac{p^2}{p^4-1}\left[\frac{2p^2-1}{p\sqrt{p^2-1}}\ln(p+\sqrt{p^2-1}) - 1\right] \quad (7)$$

At high axial ratio, placement of frictional elements with their centers on the surface will increase a_2 relatively much more than a_1. Neglecting the change in the slowly varying $y(p)$, then

$$(\zeta_r)_{eff} \approx (\zeta_r)_0(1 + \beta' r/a_2)^2 \quad (8)$$

In other words, the proper method of extrapolation may depend on particle shape. In the work reported here, linear and quadratic extrapolations have usually been employed, and $D^{\theta\theta}$ has been extrapolated rather than ζ_r. Cubic extrapolations have not proved satisfactory, presumably because of point scatter. Generally, the result of the quadratic extrapolation has been preferred

except in cases of high point scatter where the linear extrapolation is clearly more reliable. Since different values are obtained by different extrapolations, an uncertainty of a few per cent must be attached to most of the reported values.

Results

Spheres. A computer program was written which placed small spherical modelling elements in parallel bands on a spherical surface of radius R_0. One element was placed at the north pole, and an integral number of bands were placed between the polar element and the equator. The frictional element radius r was chosen to make each element tangent to its upper and lower band boundaries. The maximum integral number of elements, evenly spaced, were placed in each band. Except in the band immediately below the pole element, the first element in each band was placed below and halfway between the first and second elements of the band above it. The elements in the lower hemisphere were placed by inversion through the center. This procedure introduced a symmetry which was useful in reducing the number of computer calculations.

The results of the calculation, carried out on the University of Illinois IBM 7094 computer, are given in Table I. Within the limits of uncertainty in the extrapolation, it is clear that the shell model gives the correct value for the rotational diffusion of a sphere.

TABLE I: Rotational Diffusion of a Sphere Represented by the Shell Model.

r/R_0	No. of Frictional Elements	$D^{\theta\theta}_{\text{calcd}}/D^{\theta\theta}_{\text{exact}}$	Residuals (linear extrapolation)
0.1736	98	0.868	-2.8×10^{-3}
0.1205	208	0.908	1.0×10^{-2}
0.0923	358	0.929	-1.1×10^{-2}
0.0747	550	0.942	3.5×10^{-3}
0.0		0.998	(linear extrapolation)
0.0		0.999	(quadratic extrapolation)

Bloomfield *et al.* (1967) have shown that the translational properties of an assembly of frictional elements representing a particle are not appreciably affected by the random removal of elements until a large fraction of the elements have been removed. That is, there is little free draining through an assembly of frictional elements even when the assembly has gaps or holes. A simple estimate of the effect of draining in rotational motion may be made in the following way. For an assembly such as that used in the calculations reported in Table I, the frictional element radius r is progressively reduced *without* changing the number or positions of the elements. The new frictional element radius may be represented as ξr, where $\xi \leq 1$. The shrinking of the frictional elements results in an increasingly open assembly with more and more draining. At the same time, since the frictional elements are becoming smaller, they do not extend out so far from the surface. These two factors both act to decrease ζ_r, and at some value ξ_{cr} the assembly of shrunken frictional elements will have the same value of ζ_r as the shell model.

The result of one such calculation is given in Table II.

TABLE II: The Effect of Shrinking Frictional Elements in Place.

$r/R_0 = 0.0923$	
ξ	$D^{\theta\theta}_{\text{calcd}}/D^{\theta\theta}_{\text{exact}}$
0.3	1.071
0.4	1.020
0.5	0.990
0.6	0.970
0.7	0.955
0.8	0.944
0.9	0.936
1.0	0.929

These data show that for a spherical particle $\xi_{cr} \approx 0.48$, at which point less than 24% of the surface is covered. It is apparent that the structure must be quite open before draining becomes at all important. It has also been shown, in calculations not reported here, that ξ_{cr} for spheres is essentially independent of the initial value of r/R_0.

Prolate Ellipsoids of Revolution. A computer program was written for prolate ellipsoids very much like that for spheres, except that in the absence of accurate analytical expressions which could be solved directly for the placement of frictional elements, it was necessary to place the bands on the ellipsoid surface by an iterative procedure. The results of the calculations, extrapolated to zero radius of the modelling element, are given in Table III. Since prolate ellipsoids of axial ratio greater than 10 or so require a very large number of frictional elements for adequate modelling, and therefore computer time becomes excessively long, it was not found practical to go to higher axial ratios. A single assembly was created for an axial ratio of 15, using 822 elements, and the rotational diffusion coefficient of this assembly was determined, but no extrapolation to a continuous surface distribution was attempted. The Perrin (1934) expressions (eq 6 and 7) were used to determine $D^{\theta\theta}_{\text{exact}}$.

It is interesting that the calculated value of the rotational diffusion coefficient is too large for all axial ratios. The discrepancy rises to a maximum value of over 8% at an axial ratio of 6, and seems to level off at about 8% for higher axial ratios. Similar behavior was found by

TABLE III: Rotational Diffusion of Prolate Ellipsoids. Shell Model Representation.

Axial Ratio	$D^{\theta\theta}_{calcd}/D^{\theta\theta}_{exact}$ Linear Extrapolation	Quadratic Extrapolation
2.0	1.028	1.005
4.0	1.060	1.078
5.0	1.066	1.052
6.0	1.086	1.166
7.0	1.085	0.883
8.0	1.062	1.463
10.0	1.078	1.136
15.0	1.078 (unextrapolated)	

Bloomfield *et al.* (1967) for translation. No explanation has yet been found for this discrepancy.

It is seen in Table III that linear extrapolations were much less erratic than quadratic ones, presumably because of point scatter owing to very inefficient coverage of the ellipsoidal surface near the poles at higher axial ratios. With a larger number of points, quadratic extrapolation might become more useful.

For each axial ratio, the value of the critical shrinking factor ξ_{cr} was estimated in the same way as was done for spheres. The results are given in Table IV. Allowing for

TABLE IV: ξ_{cr} as a Function of Axial Ratio p for Prolate Ellipsoids.

p	ξ_{cr}
1	0.48
2	0.48
4	0.53
5	0.60
6	0.56
7	0.59
8	0.77
10	0.80

a fair amount of scatter in the data from which these values were obtained, it seems that ξ_{cr} is a slowly increasing function of axial ratio.

Tobacco Mosaic Virus. The structure and properties of TMV have been extensively investigated, as summarized in two recent reviews (Klug and Caspar, 1960; Caspar, 1963). It is a rodlike virus containing about 2130 identical protein subunits and a single strand of RNA. There is a solvent-filled hole 40 A in diameter down the center of the rod. The maximum diameter of the rod is 180 A, but the regular grooves between the helically arranged protein subunits permit adjacent virus particles in oriented gels to approach each other more closely by means of an interlocking fit. In such gels, the spacing between the axes of adjacent particles is observed to be 150 A, and this is the diameter which is often given for the virus. The electron microscopic study of Hall (1958) led to a value of 3020 ± 50 A for the virus length. The rotational diffusion coefficient has been determined by transient electric birefringence (O'Konski and Haltner, 1956) to be 333 ± 13 sec^{-1}, while flow birefringence studies (Boedtker and Simmons, 1958) gave a value of about 380 sec^{-1}.

We have modelled TMV in a number of ways, all of which gave similar results for $D^{\theta\theta}$. That which most closely represents the actual structure of TMV is a stack of 116 rings of 16 spheres, each sphere 14.69 A in radius, with successive rings rotated about the cylinder axis by 11.25° to permit close packing. The outside diameter of each ring was 180 A, and the over-all length of the model was 3002 A. $D^{\theta\theta}$ calculated for this model was 410 sec^{-1}; that for a similar model in which additional frictional elements were placed to close off the ends was 399 sec^{-1}. Quadratic extrapolation to a continuous shell model with open ends gave 392 sec^{-1}; with closed ends, 370 sec^{-1}. Agreement with experimental results is seen to be reasonable. A continuous shell model of diameter 150 A gives 421 sec^{-1}. Calculations according to the Burgers (1938) and Broersma (1960) equations for the rotational frictional coefficients of cylinders, using dimensions 180 × 3000 A, gave 441 and 316 sec^{-1}, respectively. The Perrin (1934) eq 6 and 7 give $D^{\theta\theta}$ = 489 sec^{-1} for a prolate ellipsoid of minor axis 180 A and major axis 3000 A.

We have noted above that shell model calculations of $D^{\theta\theta}$ for prolate ellipsoids yield results about 8% too high, as shown in Table II. If the same discrepancy exists for cylinders, which has not been demonstrated, then the "correct" $D^{\theta\theta}$ for TMV is 410/1.08 or 380 sec^{-1}, in striking agreement with the result of Boedtker and Simmons (1958). On the other hand, closing the ends, predicted by Broersma (1960) to decrease $D^{\theta\theta}$ by 15%, is seen from these calculations to effect only about a 5% reduction.

The value of ξ_{cr} obtained for TMV modelled as a cylinder with open ends was 0.38. For a cylinder with closed ends, ξ_{cr} was found to increase regularly with decreasing r from 0.48 to 0.66, a trend perhaps related to the difficulty in covering the ends completely and evenly with elements of arbitrary size.

T2 Bacteriophage. Maestre (1966) has recently reported that T2 bacteriophage in solution shows two distinct rotational diffusion coefficients: 555 ± 54 and 111 ± 22 sec^{-1}. These may be attributed to the "fast" and "slow" forms first observed in sedimentation (Hook *et al.*, 1946; Sharp *et al.*, 1946). The structure of T2 phage, as observed in electron micrographs (Brenner *et al.*, 1959), is shown schematically in Figure 1. Actually there are six tail fibers rather than the four drawn, and they are somewhat kinked near the middle.

The differences in s and $D^{\theta\theta}$ between these forms have been attributed to extension of the tail fibers (Maestre, 1966; Bendet *et al.*, 1957, 1958; Lauffer and Bendet,

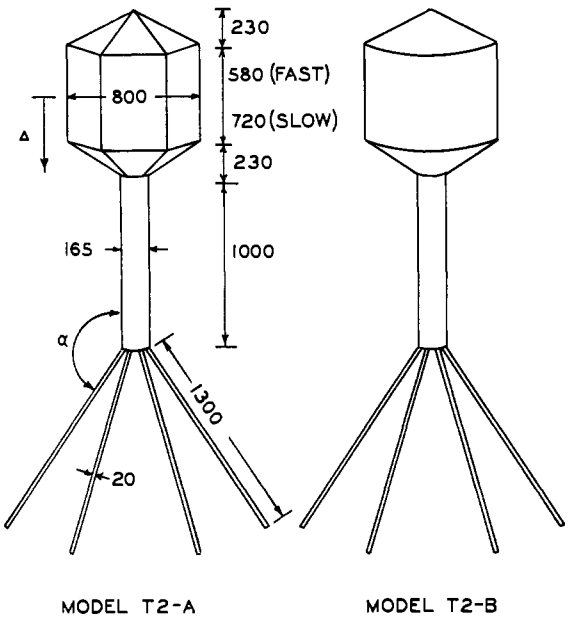

FIGURE 1: Models of T2 bacteriophage used in the calculation of $D^{\theta\theta}$. Dimensions in angstroms.

1962), and to a difference in permeability of the heads of the two forms (Cummings and Kozloff, 1960, 1962; Cummings, 1963). However, it has been shown (Bloomfield *et al.*, 1967) that neither of these explanations can account for the 40% difference in s. In this circumstance, it was suggested (Bloomfield *et al.*, 1967) that the virus particle, particularly the slow form, must shrink on dehydration during preparation for electron microscopy, so that the measured dimensions are too small. The measured $D^{\theta\theta}$'s can shed additional light on the dimensions of these forms.

The head dimensions of model T2-A in Figure 1 are essentially those reported by Cummings and Kozloff (1960). The tail and tail fiber dimensions are those obtained by Brenner *et al.* (1959). The tail diameter is that of the extended sheath, and the tail length includes the hexagonal base plate which appears in the electron micrographs at the end of the tail. The tail is attached to the head where the tail and head diameters are equal.

In the program utilizing model T2-A, frictional elements were placed in parallel, nonoverlapping bands on the head and tail. The top band (at the head apex) always contained one element. Every other band had at least six elements. The tail fibers were modelled as strings of 20-A beads. Model T2-B was utilized in a general program applicable to any tadpole-shaped phage particle, with or without tail fibers. The program was written to read in all of the phage dimensions, as well as the number and disposition of fibers, as data at the time of program execution. Frictional elements are placed in much the same way as with model T2-A, but the cylindrical head of T2-B permits a considerable reduction in computer time due to its higher symmetry.

In the evaluation of $D^{\theta\theta}$ by eq 1, it is necessary to refer the coordinates n_s to the center of frictional resistance (Zimm, 1956), whose position is not known *a priori*. This is the point about which rotation is easiest. The following method was devised for the location of that point. A provisional particle-fixed coordinate system is defined with the origin at the center of the head. For any frictional element the l and m coordinates can now be given. These coordinates will not change as the origin is moved along the axis of symmetry. The n coordinate of the element may be given as $(n + \Delta)$, where n is the coordinate in the original provisional coordinate system and Δ is the distance through which the origin is moved toward the tail. Equation 1 may now be rewritten as

$$\frac{D^{\theta\theta}}{kT} = \frac{1}{(\alpha + \beta)\zeta}\left\{1 + \frac{\zeta}{8\pi\eta_0(\alpha + \beta)}(T_1 + T_2\Delta + T_3\Delta^2)\right\} \quad (9)$$

where

$$\beta = U_1 + U_2\Delta + U_3\Delta^2 \quad (10)$$

$$U_1 = \sum_{s=1}^{N} n_s^2, \qquad U_2 = 2\sum_{s=1}^{N} n_s \quad (11)$$

where $U_3 = N$ = total number of elements and

$$T_1 = \sum_{s=1}^{N}\sum_{t=1}^{N}{}'\left[\left\langle\frac{l_s l_t}{R_{st}}\right\rangle + \left\langle\frac{n_s n_t}{R_{st}}\right\rangle + \left\langle\frac{(l_s n_t - n_s l_t)^2}{R_{st}^3}\right\rangle\right] \quad (12)$$

$$T_2 = \sum_{s=1}^{N}\sum_{t=1}^{N}{}'\left[\left\langle\frac{n_s + n_t}{R_{st}}\right\rangle + \left\langle\frac{2(l_s - l_t)(l_s n_t - n_s l_t)}{R_{st}^3}\right\rangle\right] \quad (13)$$

$$T_3 = \sum_{s=1}^{N}\sum_{t=1}^{N}{}'\left[\left\langle\frac{1}{R_{st}}\right\rangle + \left\langle\frac{(l_s - l_t)^2}{R_{st}^3}\right\rangle\right] \quad (14)$$

It is apparent that U_1, U_2, U_3, T_1, T_2, and T_3 can be evaluated for any given assembly in a single time-consuming computation after which Δ can be varied extensively, with very little increase in computer time, to give $D^{\theta\theta}$ as a function of Δ. This function can be examined to find the value of Δ which gives the maximum value of $D^{\theta\theta}$ and hence the true rotational center of the particle. The computer may perform this task conveniently by generating an extensive table of (Δ, $D^{\theta\theta}$) data points, searching the table for the maximum value of $D^{\theta\theta}$ listed, fitting the points in that part of the table with a quadratic function, and then differentiating the function to locate the maximum.

Another problem arises from the number of frictional elements required to adequately model the T2 particle. Since the tail fiber diameter is 20 A, this is the maximum diameter for the spherical elements. If the entire particle

is to be modelled with 20-A spheres, a total of 7699 spheres will be required (model T2-A, fast form). The double sum of eq 1 requires a number of computer calculations proportional to the square of the number of elements. Thus, if an assembly of 500 elements requires 1 min for calculation, an assembly of 7699 elements would require $(7699/500)^2$ or 237 min, so that a direct calculation is to be avoided if possible. In order to bring computation time down to about 10 min for this case, two stratagems have been employed.

The first of these stratagems takes note of the fact that all but 390 of these 7699 elements are in the head and tail. In other words, the vast majority of the terms in the double sum (and in α and β) are head–head, tail–tail, head–tail, and tail–head terms. The head and tail alone can be adequately modelled with spheres larger than 20 A. Thus the problem is to find the variation of the double sum (DSM) and of $(\alpha + \beta)$ with r at a given value of Δ. It can be shown analytically that for spherical particles $(\alpha + \beta)$ is proportional to the surface density of elements, that is to r^{-2}. The terms $\sum_s \sum_t{}' (l_s l_t / R_{st})$ and $\sum_s \sum_t{}' (n_s n_t / R_{st})$ are both proportional to the square of the surface density of elements, that is to r^{-4}. One would expect that $\sum_s \sum_t{}' [(l_s n_t - n_s l_t)^2 / R_{st}^3]$ would also be proportional to r^{-4}. In other words, for spheres and hopefully for other particles as well

$$(\alpha + \beta) r^2 \approx \text{constant} \tag{15}$$

$$\text{DSM} r^4 \approx \text{constant} \tag{16}$$

This approach was tested on the model of T2 phage without fibers, by comparing values of $(D^{\theta\theta}\eta/kT)_{r=0}$ obtained by separate extrapolation of $(\alpha + \beta)r^2$ and $\text{DSM}r^4$ to $r = 0$, with continuous shell model values of $(D^{\theta\theta}\eta/kT)$ obtained in the usual way. A discrepancy of a per cent or so was found, as well as some uncertainty in the location of the rotational center, but these are acceptable errors.

TABLE V: Rotational Diffusion of T2 Phage and Its Parts. Model T2-A.

α	$D^{\theta\theta}_{20,w}$, fast (sec^{-1})	Δ (A)	$D^{\theta\theta}_{20,w}$, slow (sec^{-1})	Δ (A)
Head	1986			
Tail	5007			
Fiber	6628			
Head and tail	787	408	623	415
Whole virus				
$\pi/4$	617	483	529	502
$\pi/2$	508	564	440	586
$3\pi/4$	419	643	368	665
$9\pi/10$	395	666	348	690
Experimental (Maestre, 1966)	555 ± 54		111 ± 22	

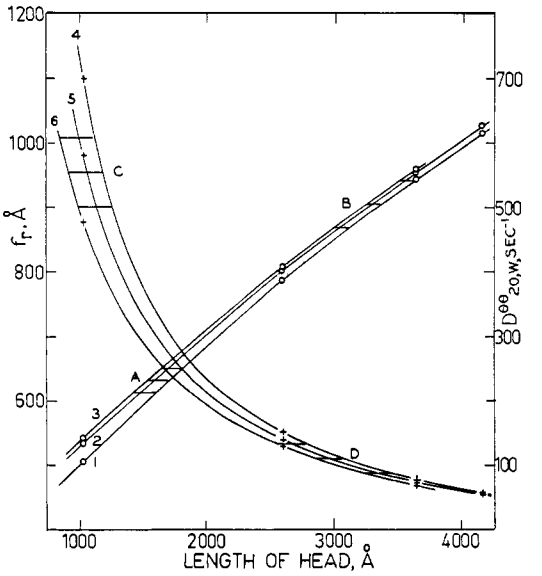

FIGURE 2: The effect of a longitudinal expansion of the T2 head. Model T2-B: head diameter 800 A, apex height 230 A, tail diameter 165 A, and tail length 1000 A. O and + are calculated points. Key to symbols used in Figures 2–5:

	f_r	$D^{\theta\theta}_{20,w}$,
Fibers not extended	1	4
Fibers extended $\alpha = \pi/4$	2	5
$\alpha = \pi/2$	3	6
Experimental values		
fast form	A	C
slow form	B	D

Horizontal lines above and below A–D represent experimental uncertainty.

The second simplifying device used to reduce the number of computer calculations takes advantage of the symmetry of the model. In model T2-A, there are six fibers and six head faces. Furthermore, the number of elements in each band around the tail was reduced from the maximum of 25 (with r = 10 A) to 24. Thus the model has sixfold symmetry. By a series of transformations which need not be detailed here, this symmetry was used to reduce the number of calculations by a factor of 6.

The results obtained for T2 phage using model T2-A are given in Table V. It is clear that even complete extension of tail fibers does not reduce $D^{\theta\theta}$ to the observed value for the slow form, and that in fact the presence of tail fibers in the fast form is necessary to bring $D^{\theta\theta}$ down to the experimental value. It was accordingly attempted to find virus dimensions that would give the correct frictional properties for both forms.

An initial investigation established two points. The first is that moderate variations in tail diameter are unimportant. Increasing the diameter from 165 to 200 A effected a decrease in $D^{\theta\theta}$, when $\alpha = \pi/4$, from 579 to

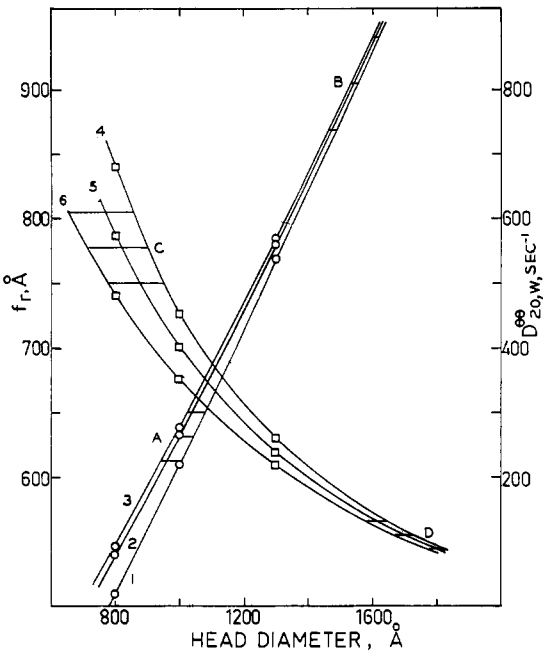

FIGURE 3: The effect of a uniform expansion of the T2 head. Model T2-B: tail diameter 200 A and tail length 1000 A. O and □ are calculated points.

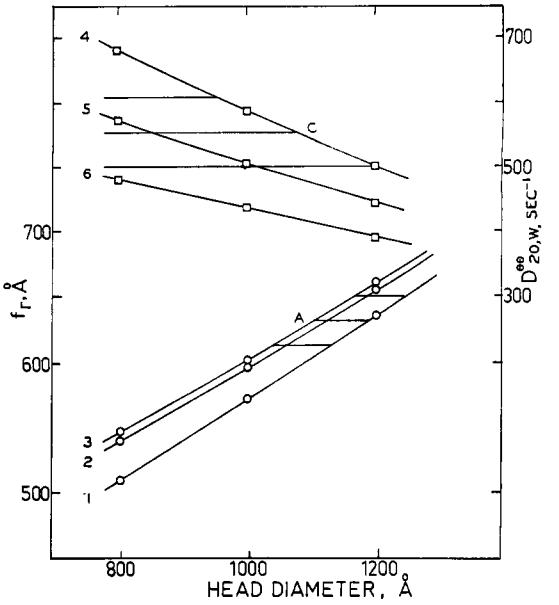

FIGURE 4: The effect of a lateral expansion of the T2 head. Model T2-B: head length 1040 A, tail diameter 200 A, and tail length 1000 A. O and □ are calculated points.

574 sec^{-1}. This change is clearly insignificant, and probably lies within the uncertainty of the extrapolation. This result was to have been expected, because of the dominant influence of the head on the hydrodynamic properties. The second point is that models T2-A and T2-B have similar hydrodynamic properties. The ratio $D^{\theta\theta}{}_{T2-A}/D^{\theta\theta}{}_{T2-B}$ was 1.240 for heads alone; 1.128 for head and tail; and 1.067 for the whole virus with fibers at $\alpha = \pi/2$. A ratio of about 1.240 for heads alone was to have been expected, since the T2-B head has a larger volume. However, addition of tail and fibers brings the ratio down to a value sufficiently close to unity that the greater symmetry of model T2-B, which in parts of the program permits reduction of the number of calculations by a factor of several hundred, may be used to advantage.

With these points established, it was possible to proceed to a systematic variation of model size in order to determine those dimensions which would secure agreement with the experimental data. It was assumed that only the head dimensions need be varied. This assumption was suggested by the electron micrographs of Cummings and Kozloff (1960), and in any case it seemed reasonable from a practical point of view, since the head dominates the hydrodynamic properties of the phage.

To begin with the head was varied in two different ways: by a longitudinal expansion along the axis only, in accordance with the observations of Cummings and Kozloff, and by a uniform expansion without any change in head proportions. Translational frictional radii $f_r = f/6\pi\eta_0$ (Bloomfield *et al.*, 1967) and rotational diffusion coefficients were calculated for several head sizes in both modes of expansion. The results are shown in Figures 2 and 3. Experimental translational frictional radii of 632 and 905 A for the fast and slow forms, respectively, were calculated from the sedimentation and

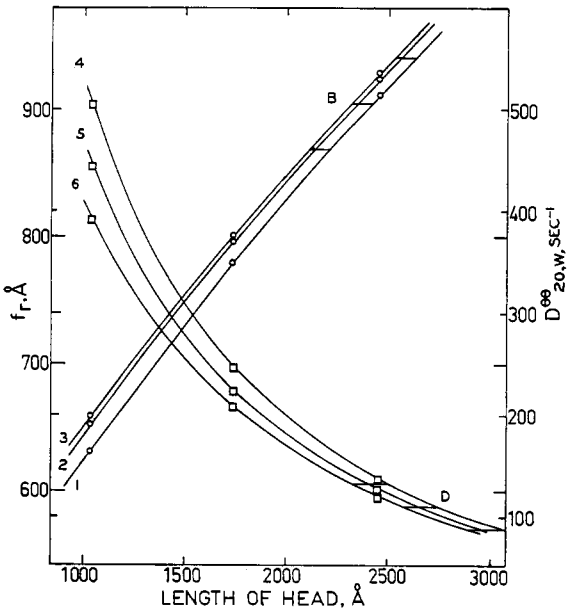

FIGURE 5: The effect of a subsequent longitudinal expansion of the T2 head. Model T2-B: head diameter 1190 A, apex height 230 A, tail diameter 200 A, and tail length 1000 A. O and □ are calculated points.

diffusion data of Cummings and Kozloff (1960) using the partial specific volume obtained by Taylor (1946).

Unfortunately, neither the longitudinal nor the uniform modes of expansion can provide head dimensions which simultaneously account for f_r and $D^{\theta\theta}$ of the fast form. For example, if the head dimensions are adjusted to give the experimental frictional radius of 632 A with $\alpha = \pi/2$, $D^{\theta\theta}$ is calculated to be 283 sec^{-1} for longitudinal expansion and 362 sec^{-1} for uniform expansion, compared to 555 sec^{-1} for experimental. This discrepancy is considerably greater in the former case, suggesting that better agreement might be obtained if longitudinal changes in the head were minimized. On the other hand, the longitudinally expanded model shows better agreement for the slow form. The obvious conclusion is that agreement with all of the experimental data might be approached if the head were first expanded *laterally* to an overall frictional radius of 632 A, then *longitudinally* to an overall frictional radius of 905 A. It should be noted, however, that there is no other evidence supporting this picture of the expansion, and the electron micrographs of Cummings and Kozloff (1960) argue against it.

Calculations made for this two-step method of expansion led to the results shown in Figures 4 and 5. Exact agreement with translational data for the fast form was achieved with head dimensions of 1040 × 1190 A, fibers not extended. These dimensions gave simultaneous, though marginal, agreement with the rotational data. Subsequent longitudinal expansion, holding the head diameter constant at 1190 A, led to reasonably good simultaneous agreement with translational and rotational data for the slow form with head dimensions of 2310 × 1190 A, tail fibers extended at an angle $\alpha = 3\pi/4$. It might be noted that if the head diameter were made slightly smaller than 1190 A for both forms, it would be possible to improve the agreement with rotational data without introducing undue disagreement with the translational data.

It should be remembered that the dimensions quoted are for the T2-B representation. The maximum head diameter of the corresponding T2-A representation will, of course, be somewhat larger.

Discussion

It may be concluded from these results that the "shell model" method of calculating rotational diffusion coefficients for complex structures is both computationally feasible and sufficiently accurate. For asymmetric structures such as prolate ellipsoids, $D^{\theta\theta}$ calculated from the shell model may be off by as much as 8% from the exact result. However, this discrepancy is not far from the range of experimental uncertainty in many determinations of rotational diffusion coefficients, and will only cause an error of about 3% in the estimation of polymer dimensions. It seems worthwhile remarking on the empirical observation, which is thus far without theoretical justification, that rather coarse modelling of spheres, ellipsoids, and rods by frictional elements of radius 20% or more of the small dimension of the particle, followed by shrinkage of the elements by a factor $\xi = 0.5$, gave in all cases investigated a value of $D^{\theta\theta}$ which was no more than 6% off from the shell model value. This circumstance permits very substantial savings in computer time.

The calculations on TMV do not lead to any definite conclusions regarding the importance of end effects in cylindrical particles. The theory of Broersma (1960), in which additional end effects are introduced, leads to considerably better agreement with the experimental results of O'Konski and Haltner (1956) than does the shell model. The shell model calculations, on the other hand, are in better accord with the results of Boedtker and Simmons (1958). Uncertainties in the length and hydrodynamic diameter of TMV particles also hinder comparison of theory and experiment.

Application of these methods of calculating hydrodynamic properties to T2 bacteriophage has indicated that the observed differences between the slow and fast forms cannot be attributed to tail fiber disposition or head permeability. Instead, substantial changes in head size and/or shape must be involved. It would be very desirable, of course, to check this conclusion by non-hydrodynamic methods in solution, such as light scattering.

One might ask whether, with head sizes as large as those indicated for the slow form, there is enough protein to cover the head surface. Cummings (1963) has determined that the head protein consists of about 1800 monomers of mol wt 42,000 and ellipsoidal dimensions 270 × 19 × 19 A. If the long axis of the ellipsoid were to lie in the plane of the surface, the area covered by the ellipsoid itself would be $\pi(135)(9.5)$ or 4029 A^2. If the ellipsoidal subunits were arranged side by side in rows, each ellipsoid would be assigned a rectangular area of (270)(19) or 5130 A^2. The total area covered by 1800 monomers would, therefore, lie between 7,250,000 and 9,230,000 A^2. If the head dimensions of the slow form are 3250 × 800 A (those obtained by a longitudinal expansion), the total surface area of the head in the T2-B representation is 8,170,000 A^2 which is in the calculated range. Apparently there is enough protein to cover the head surface, even in the slow form. The protein coat would be thin and presumably quite permeable to solvent, in accordance with the observations of Cummings and Kozloff (1962).

Acknowledgments

We wish to acknowledge very helpful discussions with Dr. W. O. Dalton and Professor K. E. Van Holde.

References

Bendet, I. J., Allison, J. L., and Lauffer, M. A. (1958), *Virology 6*, 571.

Bendet, I. J., Swaby, L. G., and Lauffer, M. A. (1957), *Biochim. Biophys. Acta 25*, 252.

Bloomfield, V. A., Van Holde, K. E., and Dalton, W. O. (1967), *Biopolymers 5*, 149.
Boedtker, H., and Simmons, N. S. (1958), *J. Am. Chem. Soc. 80*, 2550.
Brenner, S., Streisinger, G., Horne, R. W., Champe, S. P., Barnett, L., Benzer, S., and Rees, M. W. (1959), *J. Mol. Biol. 1*, 281.
Broersma, S. (1960), *J. Chem. Phys. 32*, 1626.
Burgers, J. M. (1938), 2nd Report on Viscosity and Plasticity, Amsterdam Academy of Sciences, Amsterdam, Nordemann, Chapter 3.
Caspar, D. L. D. (1963), *Advan. Protein Chem. 18*, 37.
Cummings, D. J. (1963), *Biochim. Biophys. Acta 68*, 472.
Cummings, D. J., and Kozloff, L. M. (1960), *Biochim. Biophys. Acta 44*, 445.
Cummings, D. J., and Kozloff, L. M. (1962), *J. Mol. Biol. 5*, 50.
Gans, R. (1928), *Ann. Physik* [4] *86*, 628.
Hall, C. E. (1958), *J. Am. Chem. Soc. 80*, 2556.
Hearst, J. E. (1963), *J. Chem. Phys. 38*, 1062.
Hook, A. E., Beard, D., Taylor, A. R., Sharp, D. G., and Beard, J. W. (1946), *J. Biol. Chem. 165*, 241.
Kirkwood, J. G. (1949), *Rec. Trav. Chim. 68*, 649.
Kirkwood, J. G. (1954), *J. Polymer Sci. 12*, 1.
Klug, A., and Caspar, D. L. D. (1960), *Advan. Virus Res. 7*, 225.
Lauffer, M. A., and Bendet, I. J., (1962), *Biochim. Biophys. Acta 55*, 211.
Maestre, M. F. (1966), *Polymer Preprints 7*, 1163.
O'Konski, C. T., and Haltner, A. J. (1956), *J. Am. Chem. Soc. 78*, 3604.
Perrin, F. (1934), *J. Phys. Radium* [7] *5*, 497.
Perrin, F. (1936), *J. Phys. Radium* [7] *7*, 1.
Riseman, J., and Kirkwood, J. G. (1956), *in* Rheology, Vol. I, Eirich, F., Ed., New York, N. Y., Academic, Chapter 13.
Sharp, D. G., Hook, A. E., Taylor, A. R., Beard, D., and Beard, J. W. (1946), *J. Biol. Chem. 165*, 259.
Taylor, A. R. (1946), *J. Biol. Chem. 165*, 271.
Zimm, B. H. (1956), *J. Chem. Phys. 24*, 269.

Spectroscopic Studies on Spinach Ferredoxin and Adrenodoxin*

Graham Palmer, Hans Brintzinger, and Ronald W. Estabrook

ABSTRACT: Two non-heme iron proteins, adrenodoxin and spinach ferredoxin, which are similar to each other in many respects but differ in that their electron paramagnetic resonance (epr) signals are axially symmetric and rhombic, respectively, have been investigated for their optical activity, in order to characterize further the symmetry of the ligand field of iron in these proteins. Circular dichroism spectra of the oxidized and reduced proteins were obtained from 700 to 300 mμ and analyzed in terms of individual Gaussian components. Unexpectedly, it was found that the optical activity of the two proteins is very similar, differing only by minor shifts in wavelength and intensity of the individual components, and by the occurrence of weak additional bands at the fringes of the spectra of ferredoxin.

Low-temperature optical spectra of the proteins are given.

In recent years there has been increasing interest in a new family of iron proteins in which iron is not a component of heme, but rather appears to be bonded directly to the protein. Although there are numerous proteins which would nominally belong in this class, *e.g.*, ferritin, conalbumin, rubredoxin, the designation non-heme iron protein (NHIP),[1] as this new group of proteins has unfortunately been labeled, is usually only applied to those iron proteins which liberate H_2S on acid denaturation, *i.e.*, those which contain acid-labile sulfur. Furthermore, the NHIP all exhibit characteristic optical absorption, although the visible spectra are rather plain by comparison to those obtained with the heme proteins.

Many of these NHIP are further characterized by unique magnetic resonance properties exhibiting a novel electron paramagnetic resonance (epr) signal at $g = 1.94$ after reduction. Until recently, it appeared

* From the Biophysics Research Division, Institute of Science and Technology, The University of Michigan, Ann Arbor, Michigan, and Department of Biophysics and Physical Biochemistry, Johnson Research Foundation, University of Pennsylvania, Philadelphia, Pennsylvania. *Received June 30, 1966.* Supported by U. S. Public Health Research Grants GM-12176 and GM-12202 and by U. S. Public Health Service Research Career Development Awards GM-K3-31,213 (G. P.) and GM-K3-4111 (R. W. E.).

[1] Abbreviations used: NHIP, non-heme iron proteins; TPNH, reduced triphosphopyridine nucleotide; CD, circular dichroism; epr, electron paramagnetic resonance.